Monatshefte für Chemie 132, 473–486 (2001)

Monatshefte für Chemie
Chemical Monthly

Studies on the Anode/Electrolyte Interface in Lithium Ion Batteries

Martin Winter[1,*], **Wolfgang K. Appel**[2], **Bernd Evers**[1], **Tomáš Hodal**[1], **Kai-Christian Möller**[1], **Ingo Schneider**[1], **Mario Wachtler**[1], **Markus R. Wagner**[1], **Gerhard H. Wrodnigg**[1], and **Jürgen O. Besenhard**[1]

[1] Institute for Chemical Technology of Inorganic Materials, Graz University of Technology, A-8010 Graz, Austria

[2] Aventis Research and Technologies GmbH & Co KG (former Hoechst Research and Technology Deutschland), Operative Research, D-65926 Frankfurt am Main, Germany

Summary. Rechargeable lithium ion cells operate at voltages of 3.5–4.5 V, which is far beyond the thermodynamic stability window of the battery electrolyte. Strong electrolyte reduction and anode corrosion has to be anticipated, leading to irreversible loss of electroactive material and electrolyte and thus strongly deteriorating cell performance. To minimize these reactions, anode and electrolyte components have to be combined that induce the electrolyte reduction products to form an effectively protecting film at the anode/electrolyte interface, which hinders further electrolyte decomposition reactions, but acts as membrane for the lithium cations, *i.e.* behaving as a solid electrolyte interphase (SEI). This paper focuses on important aspects of the SEI. By using key examples, the effects of film forming electrolyte additives and the change of the active anode material from carbons to lithium storage alloys are highlighted.

Keywords. Anode; Graphite; Lithium alloy; Lithium ion battery; Solid electrolyte interphase.

Introduction

Numerous rechargeable lithium cells have been developed in the last decades in order to satisfy the increasing demands for high energy density batteries for portable electronic applications. Only few of them have been successfully commercialized, the most important to date being the lithium ion battery. The high specific energies (>130 $Wh \cdot kg^{-1}$) and energy densities (>250 $Wh \cdot dm^{-3}$) of lithium ion cells make their application highly attractive. Beginning with the introduction of lithium ion cells in 1990 [1], their share in the rechargeable consumer battery market has dramatically increased over the years. The estimated world wide production was 200 million cells for 1997 [2]. Lithium ion cells play a major role in the so called "3C" market (cellular phones, portable computers, camcorders). Moreover, several

* Corresponding author

companies have announced or established a prototype production of electric vehicles equipped with large lithium ion batteries. More than 90% of the cells are manufactured in Japan. There are also strong activities in Europe and in the US to participate in this market, either by manufacture of cells or by production of battery materials. Moreover, in late 1999/early 2000 several manufacturers will be instituted in China, Korea, and Taiwan, which produce lithium ion cells at a much lower cost [3].

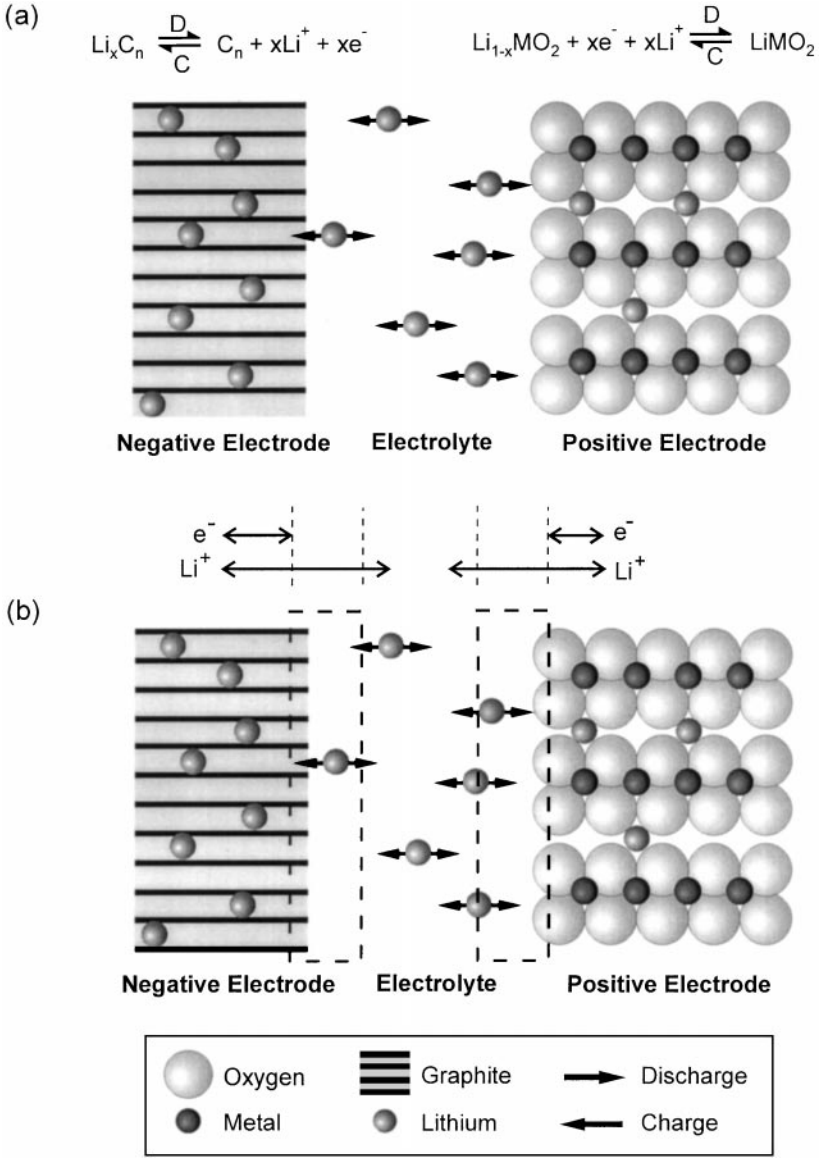

Fig. 1. (a) Schematic representation of a lithium ion cell and the charge/discharge reactions at the electrodes; as for the graphite negative electrode (anode), layered insertion electrode materials, *e.g.* $LiCoO_2$ and $LiNiO_2$, are used for the positive electrode (cathode) as well; (b) formation of electronically insulating but lithium ion conducting interphases at the electrodes

In lithium ion cells no metallic lithium is present at any state of charge/discharge. Both electrodes are capable of reversible lithium insertion (Fig. 1a). Basically, this insertion reaction is a host/guest solid state redox reaction involving electrochemical charge transfer coupled with insertion of mobile guest ions from an electrolyte into the structure of a solid host, which is a mixed electronic and ionic conductor. In commercial cells, mainly carbonaceous hosts (non-graphitic carbons or graphites) are used for the negative electrode, and lithium/transition metal oxides are employed for the positive electrode ($LiCoO_2$, $LiNiO_2$, or $LiMn_2O_4$). Because of the strong difference of the chemical potential of lithium in the two electrodes, which corresponds to cell voltages of more than 3.5 V, the transfer of lithium ions from the negative electrode through the electrolyte to the positive electrode (discharge) delivers energy whereas the reverse lithium transfer (charge) consumes energy. In view of electrochemical performance, as well as economical and ecological impacts, $LiMn_2O_4$ cathodes and graphitic anodes seem to be the preferred electrode materials for lithium ion batteries in the future. Typically, lithium salts ($LiClO_4$, $LiBF_4$, $LiPF_6$, $LiN(SO_2CF_3)_2$, *etc.*) dissolved in aprotic organic solvents, *e.g.* esters or ethers or mixtures thereof, are used as electrolytes [4, 5].

The performance of lithium ion batteries strongly depends on the type of electrode material [4]. To a first approximation, properties such as charge storage capacity (denoted as specific charge ($Ah \cdot kg^{-1}$) or charge density ($Ah \cdot dm^{-3}$)), redox potentials for lithium insertion/de-insertion, reversibility, and cycle life determine the choice of a certain material. Since the introduction of lithium ion cells to the market, the specific energy has increased by more than 30%, mostly due to the use of carbon anode materials with higher lithium storage capabilities. Many manufacturers use graphites as anode materials, which typically exhibit a maximum lithium capacity of LiC_6 ($339\,Ah \cdot kg^{-1}$/$759\,Ah \cdot dm^{-3}$ with respect to lithiated graphite and $372\,Ah \cdot kg^{-1}$/$837\,Ah \cdot dm^{-3}$ with respect to unlithiated graphite). However, there is strong interest to replace carbons by anode materials which can show even higher specific charges/charge densities. A large number of metals and intermetallics (''alloys''), such as Al, Si, Sn, Sb, ''SnSb'', $SnAg_3$ *etc.*, are capable of reversible accommodation of lithium. These lithium storage metals and alloys show very high specific charges and charge densities (*e.g.* $Li_{22}Sn_5$: $790\,Ah \cdot kg^{-1}$/$2020\,Ah \cdot dm^{-3}$) and have therefore been repeatedly suggested as anode materials for Li ion batteries [6]. Unfortunately, the uptake and release of Li is accompanied by enormous volume changes (*e.g.* from Sn to $Li_{22}Sn_5$: approx. 250% volume increase; by comparison, from graphite to LiC_6: only approx. 10% volume increase), which in the case of ordinary coarse-grained, bulky metal host materials leads to cracking and crumbling of the electrode and hence renders an application in rechargeable batteries impossible [6] (see Results and Discussion).

Lithium ion cells exhibit cell voltages of up to 4.5 V and therefore operate far beyond the thermodynamic stability window of the organic electrolytes. Electrolyte decomposition occurs at both electrodes. Fortunately, electrolyte reduction products, created *in situ* during charge, form protecting films at the negative electrode which – in the ideal case – are electronically insulating and thus hinder further electrolyte reduction but still act as a membrane for the active charge carrier, the lithium cation (Fig. 1b). In other words, these films behave as a solid electrolyte

interphase (SEI) [7][1]. Since the SEI formation is associated with the irreversible consumption of material (lithium and electrolyte), the corresponding charge loss is called irreversible capacity, C_{irr}[2]. The irreversible capacities have to be minimized because they are detrimental to both specific energy and energy density of the cell and, moreover, increase the material expenses due to the necessary excess of costly positive electrode material which is the lithium source after cell assembly. In the following we will show some basic strategies which are pursued within the special research program "Electroactive Materials" in order to reach this goal. By way of illustrative examples, special emphais will be put on new electrolyte additives and reactions taking place at the lithium storage alloy interface.

Results and Discussion

Novel electrolyte solvents and electrolyte additives

Mixed solvent electrolytes containing highly viscous ethylene carbonate (*EC*) and low viscosity dilutants such as dimethyl carbonate (*DMC*) or diethyl carbonate (*DEC*) as main solvent components are presently used in commercial lithium ion batteries comprising graphitic carbons for the anode. The structural formulae of these and other electrolyte solvents and additives reported in this study are shown in Fig. 2. *DMC* and/or *DEC* are required to get a reasonable low temperature performance of the electrolyte. *EC* is indispensable because of its excellent anode filming properties. In particular, solvent co-intercalation into graphitic anodes, which is observed in many electrolytes, can be suppressed in the presence of sufficient amounts of *EC*. The massive co-intercalation of the large solvent molecules into the interlayer gaps of the graphite matrix usually leads to a drastic volume increase (>100%) which often results in electrode destruction. Moreover, the co-intercalated solvent molecules are in contact with surfaces inside the graphite. These surfaces then also take part in the film formation process. This reaction considerably increases the undesired C_{irr} in comparison to SEI formation limited to the external graphite surfaces [4, 5].

Electrolyte additives

The use of *EC*-based electrolytes involves certain limitations in bulk electrolyte properties such as poor low-temperature conductivity and high flammability. Many research groups have therefore proposed new electrolyte components which still ensure the formation of the desired SEI, but show improved bulk electrolyte

[1] The SEI concept describes the filming behaviour observed on the Li_xC_6 negative electrode in a very basic and general way. Though the function and the formation process of the SEI in several cases seems to be more complex, the concept has been quite generally accepted due to its simplicity. The situation is different at the positive electrode. Up to now, there are only a few reports on the formation and composition of protective interphases at the positive electrode (Fig. 1b and, *e.g.* Ref. [4]), and the nature and *modus operandi* of these films is still not clear.

[2] The reversible lithium insertion, on the other hand, is called discharge capacity or reversible capacity, C_{rev}.

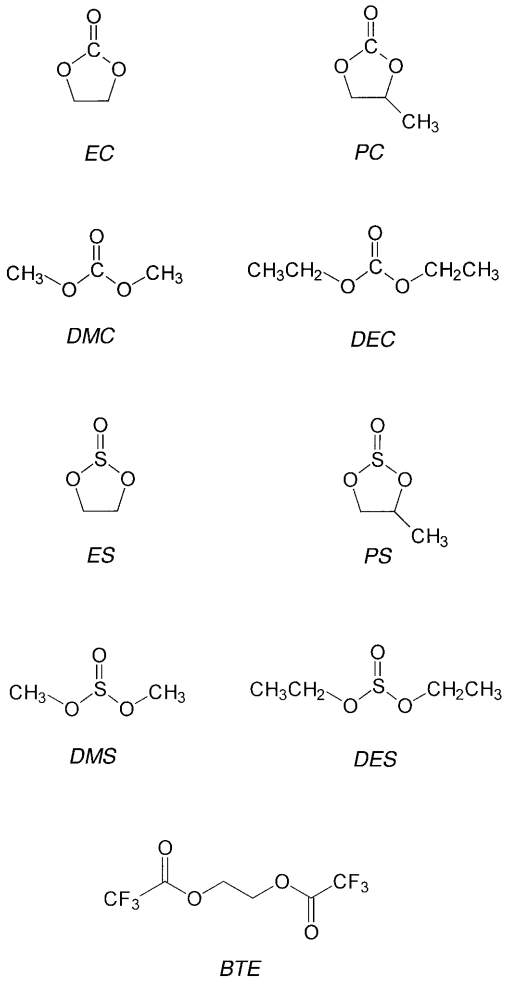

Fig. 2. Structural formulae of ethylene carbonate (*EC*), propylene carbonate (*PC*), dimethyl carbonate (*DMC*), diethyl carbonate (*DEC*), ethylene sulfite (*ES*), propylene sulfite (*PS*), dimethyl sulfite (*DMS*), diethyl sulfite (*DES*), and 1,2-*bis*-(trifluoracetoxy) ethane (*BTE*)

properties. In order to decouple the filming and bulk properties of the electrolyte, reactive electrolyte additives can be used [8, 9]. Even in small amounts these additives ensure a quick formation of the SEI, thus allowing the selection of the main electrolyte component independently of its filming properties.

The *modus operandi* of such electrolyte additives will be illustrated by ethylene sulfite (*ES*) used as an additive in a propylene carbonate (*PC*) electrolyte. Electrolytes based on *PC* are known for their better low-temperature behaviour compared to *EC* based ones. Unfortunately, strong *PC* co-intercalation into graphite takes place, which is followed by reduction of the solvated intercalates, $\mathrm{Li}(PC)_y\mathrm{C}_n$. One main reduction product is propene gas [10]. Due to *PC* co-intercalation and gas formation inside the graphite, shedding of single graphene layers or packages of graphene layers (exfoliation) occurs. Eventually, the electrode is destroyed. This process, simply called solvated intercalation, usually starts at electrode potentials of

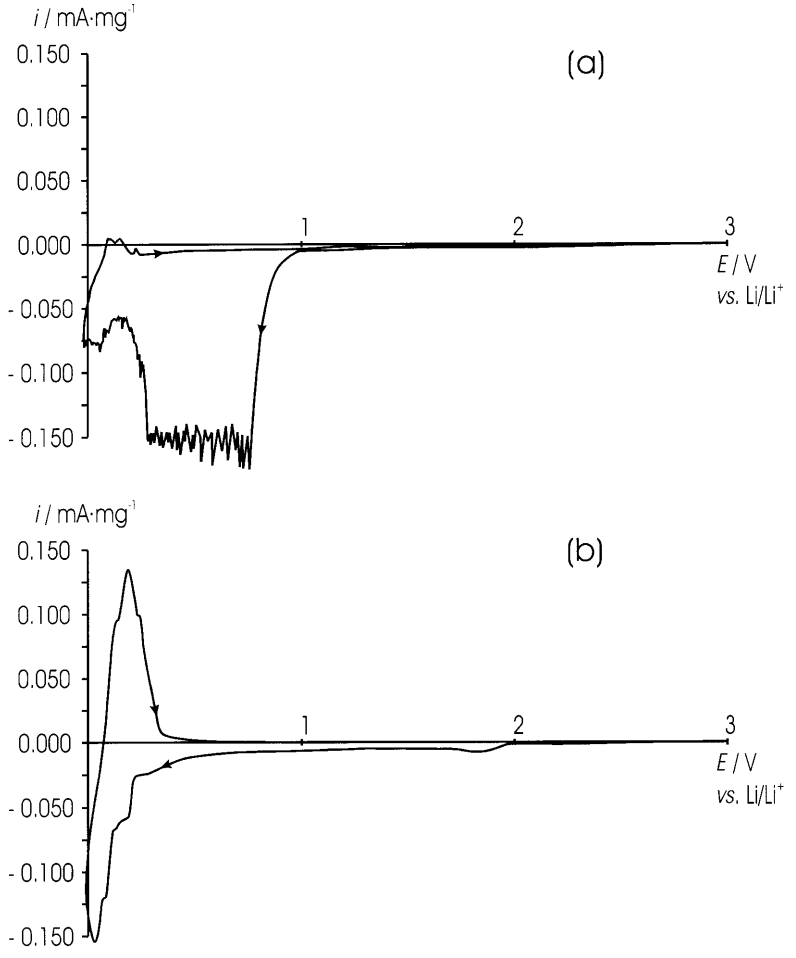

Fig. 3. (a) Cyclic voltammogram of synthetic graphite TIMREX® KS 6 in (a) 1 *M* $LiClO_4$ in *PC* and (b) 1 *M* $LiClO_4$ in *PC/ES* (95/5); scan rate: $0.05\,mV \cdot s^{-1}$

$\sim$1.0–0.9 V *vs.* Li/Li^+ (Fig. 3a). In order to assure that solvated intercalation into graphite is avoided, the formation of the SEI, which allows only Li^+-cations to pass, has to take place at potentials sufficiently far above the potentials where solvated intercalation usually occurs (Fig. 4).

The additive *ES*, which has been added in small amounts of 5% (v/v) to the *PC* electrolyte, is reduced at electrode potentials of $\sim$2.0 V *vs.* Li/L^+. The reduction products obviously form a SEI, which inhibits *PC* co-intercalation. This is confirmed by the absence of current peaks at $\sim$1 V *vs.* Li/Li^+ in the voltammogram (Fig. 3b). No exfoliation of graphite occurs. Instead, the desired reactions, intercalation and de-intercalation of unsolvated lithium, are observed at potentials of $\sim$0.3–0.0 V *vs.* Li/Li^+. Organic sulfites, whether cyclic (ethylene sulfite [8], propylene sulfite (*PS*) [11]) or linear (dimethyl sulfite (*DMS*), diethyl sulfite (*DES*) [12]) basically show a very similar filming behavior. However, the filming strength on graphitic anodes is different, *i.e.* the formation of the SEI is associated with different extents of C_{irr}. It can be estimated as follows: $ES > PS \gg DMS > DES$,

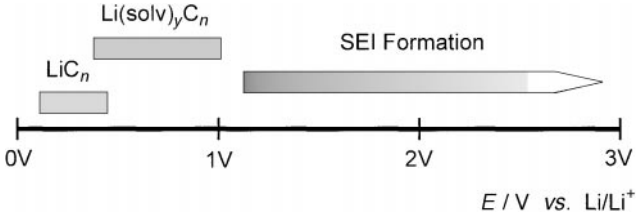

Fig. 4. Approximate potential regions for unsolvated lithium intercalation (LiC_n) and solvated lithium intercalation [$Li_x(solv)_yC_n$]; the potential region where electrolyte reduction and subsequent SEI formation should take place has to be higher than the potential region for solvated lithium intercalation

Table 1. Specific charges for charge (C_c) and discharge (C_d) as well as discharge/charge efficiencies (*Eff* = ratio of discharge capacity to charge capacity) of TIMREX® graphite SFG 44 in (a) 1 *M* $LiClO_4$ in *PC/ES* (95/5), (b) 1 *M* $LiClO_4$ in *PC/PS* (95/5), (c) 1 *M* $LiClO_4$ in *PC/DMS* (95/5), (d) 1 *M* $LiClO_4$ In *PC/DES* (95/5), (e) 1 *M* $LiClO_4$ in *PC/ES* (97/3), and (f) 1 *M* $LiClO_4$ in *PC/ES* (99.5/0.5); constant current charge/discharge cycling with $i = \pm 0.02\,A \cdot g^{-1}$, cut-off: 1.8/0.025 V *vs.* Li/Li$^+$

	Cycle Number	C_c / Ah · kg^{-1}	C_d / Ah · kg^{-1}	*Eff* / %		Cycle Number	C_c / Ah · kg^{-1}	C_d / Ah · kg^{-1}	*Eff* / %
(a)	1	429	342	79.7	(b)	1	485	338	69.7
	2	362	347	95.8		2	396	344	86.7
	3	359	350	97.7		3	389	355	91.3
	4	357	351	98.3		4	381	353	92.5
	5	353	349	98.9		5	374	355	94.9
(c)	1	555	338	61.0	(d)	1	689	301	43.7
	2	396	348	87.9		2	380	315	82.7
	3	372	342	91.9		3	356	316	88.7
	4	362	336	92.8		4	354	311	88.0
	5	364	335	92.1		5	372	305	81.9
(e)	1	425	332	78.1	(f)	1	427.5	317.3	74.2
	2	359	339	94.4		2	374.1	324.0	86.6
	3	359	341	94.9		3	364.1	324.0	89.0
	4	357	342	95.8		4	369.1	329.0	89.1
	5	352	342	97.2		5	364.1	329.0	90.5

i.e. *ES* is the most effective electrolyte additive (Table 1a–d). Even concentrations of *ES* as low as 0.5% (v/v) still enable successful cycling of graphite anodes in *PC*-based electrolytes. However, we found that the *ES* additive amount has to be in the range of 3–5% (v/v) in order to keep the discharge/charge efficiencies sufficiently high, *i.e*. to keep C_{irr} low (Table 1a,e,f).

Fluorinated solvents for lithium ion battery electrolytes

The redox potential of lithium-rich LiC_n compounds (100 mV *vs.* Li/Li$^+$) is rather close to that of metallic lithium, and the particle size of LiC_n in battery electrodes is typically in the order of ~10–40 µm, which means that the reactive surface area

with the electrolyte is large. The kinetic stability against a spontaneous reaction with the electrolyte is determined by the protective SEI [5]. In order to reach an optimum electrolyte conductivity, the electrolytes usually contain up to 66% (v/v) of the low viscosity solvents *DMC* (boiling point: 90°C, flash point: 18°C) and/or *DEC* (boiling point: 127°C, flash point: 31°C)[3]. When the protective interphases collapse, these volatile and highly flammable low viscosity components may readily react with the anode and contribute to a rapid thermal runaway of the cell[4]. A replacement of these components in future cells therefore seems inevitable.

Many partly fluorinated polar organic solvents such as ethers, esters, amides, and others show considerable solubilities for lithium salts, at least for those with large anions such as PF_6^- and $[N(SO_2CF_3)_2]^-$ [13–18], despite the strong electron-withdrawing effect of the fluorine atoms on the electron donor groups (usually containing oxygen) which are required for Li^+-ion solvation. Exchange of some hydrogen for fluorine causes significant differences in the physical and chemical properties of polar solvents. In particular, viscosities, but also melting and boiling points of fluorinated solvents, are in many cases significantly lower compared to their hydrogenated counterparts [13, 14]. Moreover, they are in general much less flammable because less hydrogen is available.

Typical examples of fluorinated organic solvents which have been investigated are glycol ethers of the type $HC_2F_4O(C_2H_4O)_nC_2F_4H$ $n = 1, 2, 3, 4, 6$ [15]), urethanes [16] such as $(CH_3)_2NCO_2CH_2CF_3$, glycol esters [17], and acetamides [18] as well as selected fluorinated carbonates, acetates, ethers, borates, and phosphates.

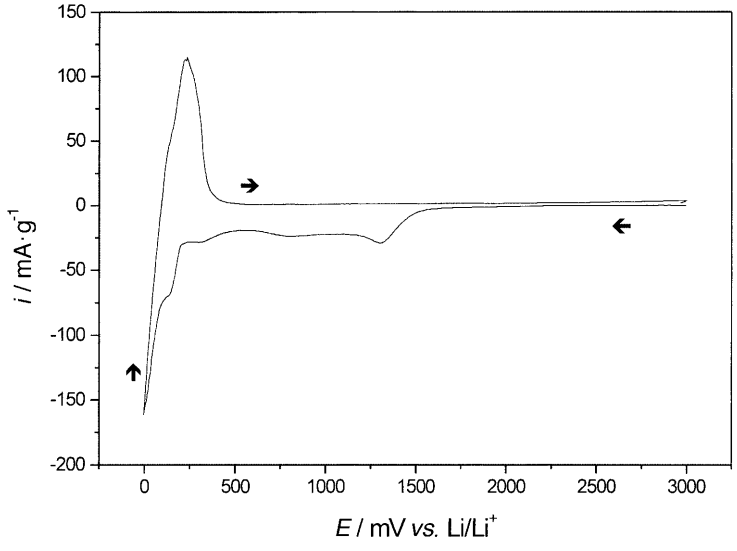

Fig. 5. Cyclic voltammogram of synthetic graphite TIMREX® KS6 in 1 *M* $LiN(SO_2CF_3)_2$ in *PC/BTE* (90/10); scan rate: 0.1 $mV \cdot s^{-1}$

[3] By contrast, *PC* and *EC* show much higher boiling and flash points (*PC*: boiling point: 240°C, flash point: 132°C; *EC*: boiling point: 244°C, flash point: 160°C).

[4] In addition, also the safety behavior at the positive electrode depends on the formation of a protective interphase and furthermore on the state of charge and the temperature conditions [4].

Table 2. Specific charges for charge (C_c) and discharge (C_d) as well as discharge/charge efficiencies (*Eff* = ratio of discharge capacity to charge capacity) of TIMREX® graphite SFG 44 in 1 *M* $LiN(SO_2CF_3)_2$ in *PC/BTE* (80/20); constant current charge/discharge cycling with $i = \pm 0.02\,A \cdot g^{-1}$, cut-off: 1.0/0.024 V *vs.* Li/Li^+

Cycle Number	C_c / $Ah \cdot kg^{-1}$	C_d / $Ah \cdot kg^{-1}$	*Eff* / %
1	358	277	77.2
2	295	285	96.6
3	291	286	98.4
4	288	285	99.0
5	296	293	99.1
6	283	282	99.7
7	287	286	99.7
8	287	287	99.7
9	283	283	99.8
10	285	285	100.0

As an example we here present data on 1,2-*bis*-(trifluoracetoxy)-ethane (*BTE* [17]; boiling point: 157°C, flash point >110°C). Like *ES* (Fig. 3b), *BTE* renders possible the operation of graphitic anodes in *PC* based electrolytes (Fig. 5). An amount as low as 10% (v/v) of the fluorinated compound in the electrolyte sufficiently suppresses *PC* co-intercalation into graphite. The SEI formation due to reduction of *BTE* starts at 1.75 V *vs.* Li/Li^+, *i.e.* at potentials higher than the potential of solvated intercalation, and thus allows reversible lithium intercalation. These observations agree with the results of the constant current charge/discharge experiments summarized in Table 2.

SEI formation on lithium storage metals and alloys

In order to overcome the problems with the mechanical disintegration of lithium storage metals and alloys during cycling (see above), several simple strategies for the design of the metallic host materials have to be followed. These strategies are summarized in the following (for more details, see Refs. [6, 19]).

(a) Proper design of particle morphology, especially particle size and porosity

(See *e.g.* Refs. [19–21]) A nano-structured material shows the same relative expansion as a polycrystalline material, but the absolute expansions are lower, and hence the cycling stability increases. Pores in the original material should offer additional space for expansion and therefore also increase the cycling stability.

(b) Incorporation of inactive components

The dilution of the active material with matrix components results in an increased cycling stability, since the reacting and expanding phase is stabilized by the non-reacting inactive matrix. This concept has first been described in detail by *Huggins et al.* [22] in the mixed-conductor matrix concept and also holds true for a number

of recently proposed promising materials, such as *Fuji*'s amorphous tin-based composite oxide [23] and tin-oxides in general (*e.g.* Ref. [24]) or materials from the Sn-Fe(-C) system [25], to mention just a few. The drawback of these active/inactive composites [25] is that the presence of inactive matrix components reduces the specific charge as well as the charge density of the electrode material.

(c) Use of multi-phase instead of single-phase materials

In multi-phase materials like *e.g.* Sn/SnSb[5] or $Sn/SnAg_3$ [19–21], the single components usually react one at a time. Hence, while one component is reacting (expanding or contracting), the other(s) do(es) not and can thus stabilize the reacting phase.

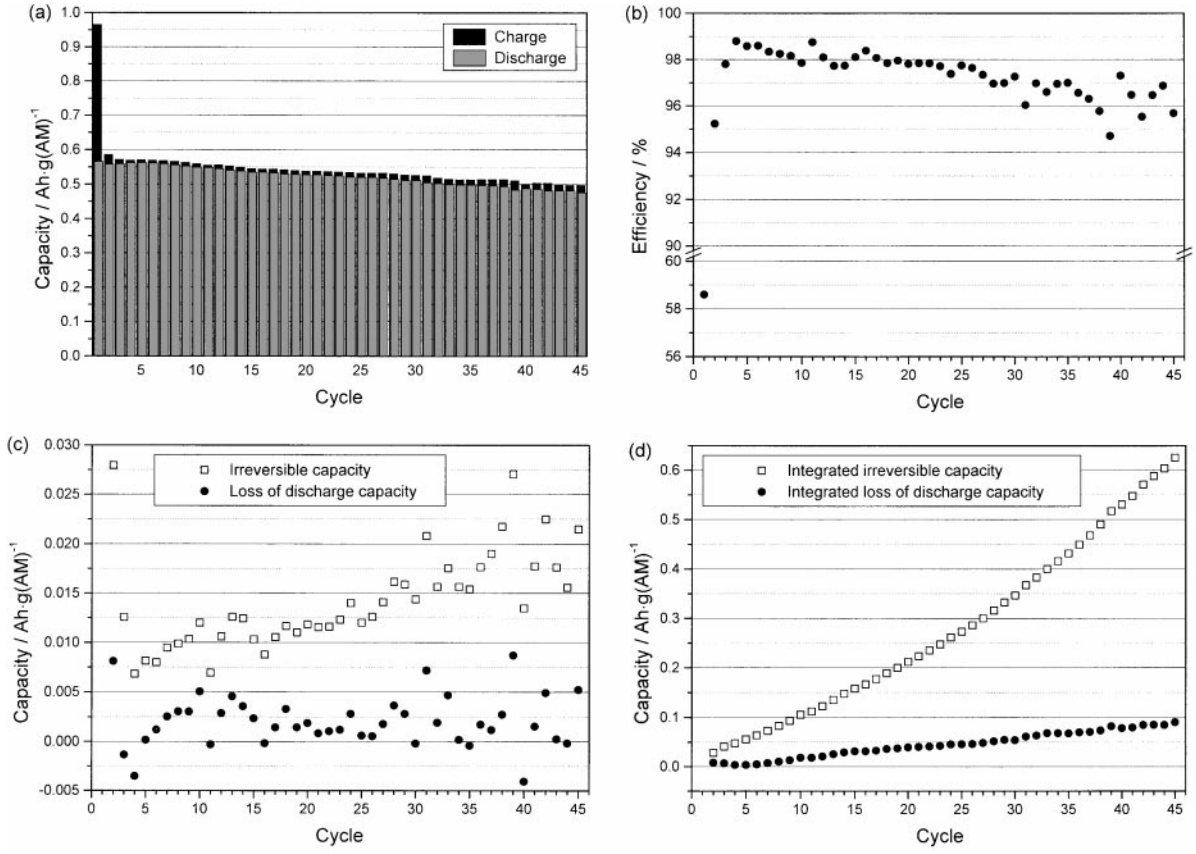

Fig. 6. Cycling performance of a Sn/SnSb composite electrode; (a) charge and discharge capacities (AM = active material), (b) efficiencies, (c) irreversible capacity and loss of discharge capacity (LDC) per cycle, (d) integrated irreversible capacity and integrated LDC (beginning with the 2nd cycle); electrolyte: 1 *M* $LiClO_4$ in *PC*; constant current charge/discharge cycling with $i = \pm 0.3 mA \cdot cm^{-2}$) (approx. $0.044 A \cdot g^{-1}$), cut-off: 1.2/0.1 V *vs.* Li/Li^+

[5] Cf. Ref. [19] for problems with the stoichiometry and structure of "SnSb".

(d) Use of components such as SnSb which show reversible phase separation and restoration upon reaction with Li [19–21]

XRD investigations of SnSb at various stages during charge point to a reaction mechanism where Li_3Sb (or $Li_{2+x}Sn_ySb$) is formed and in parallel Sn is segregated (which subsequently reacts reversibly with Li). This means that additional nano-structuring occurs *in situ*. Furthermore, this mechanism is reversible, which should at least to some extent counteract the aggregation of Sn into larger clusters during cycling (giving rise to problems with cracking and crumbling dur to the volume changes), as was found by *Courtney et al*. [26] for Sn-oxide based systems.

By following the above mentioned strategies – except point (*b*), which was avoided, since it produces additional weight and volume and thus reduces the gravimetric and volumetric lithium storage capacities of the material – it was possible to develop a composite electrode containing a nano-structured Sn/SnSb powder which shows reversible capacities of more than $500\,mAh \cdot g^{-1}$ (with respect to the mass of active material) for more than 30 cycles (Fig. 6a).

From the cycling results (Figs. 6a and b) it is evident that – apart from a further improvement of the cycling stability – future investigations will have to focus on the irreversible capacities which are high, especially in the first, but also exist in the following cycles. Some major reasons for the irreversible capacity are listed below.

(*i*) Reduction of electrolyte solution and formation of the SEI as has been discussed above for carbonaceous anodes.
(*ii*) Reduction of oxide impurities. Due to the preparation method (see Experimental), the Sn/SnSb as well as the Ni(B) powder (the latter is used as conductive electrode additive) contain oxygen impurities which will be irreversibly reduced during the first lithium uptake. This reaction should mainly occur in the first cycle.
(*iii*) Loss of contact inside the active material due to cracking and crumbling. Hence, less and less active material can partake in the charge/discharge reactions, *i.e*. the uptake and release of Li.
(*iv*) Trapping of Li in the active material, *i.e*. not all of the Li which was inserted during charge can be extracted again during discharge at the applied currents and potentials. In the case of lithium storage metals and alloys it has been frequently observed that in the cycles following the very first one the efficiencies exceed 100%. This is explained with a change in morphology (further nano-structuring during cycling, increase of porosity, *etc*.) which leads to improved kinetics (*e.g*. shorter diffusion pathways). Thus, Li which has been trapped in the initial cycle(s) may be extracted in later ones [27].

A rough estimation of the importance of the various effects is possible by comparing the irreversible capacity (C_{irr}), calculated as the difference between charge and discharge capacity, with the loss of discharge capacity (LDC) defined as the difference between the discharge capacities of two successive cycles. Since no LDC can be given for the first cycle and since the situation for the first cycle is a special one (oxide reduction, first SEI formation, first expansion), only results from cycle 2 upwards are compared in Fig. 6c (absolute values) and Fig. 6d (integrated values, beginning with the 2^{nd} cycle). Whereas all four mentioned effects are

responsible for C_{irr}, in a first approximation only loss of inter-particle contact (effect (*iii*)) and Li trapping (effect (*iv*)) should contribute to the LDC[6]. The C_{irr} values integrated from cycle 2–45 are several times larger than the integrated LDC values (Fig. 6d). Except for cycle 1, where significant surface oxide reduction can be anticipated, SEI formation is the dominating effect to C_{irr} of the metal host anodes and obviously does not diminish in the later charge/discharge cycles as in the case of graphitic anodes (cf. Table 2)[7].

Conclusions

If solvated intercalation is suppressed, graphitic carbons are dimensionally quite stable during cycling (only about 10% volume change during Li intercalation/de-intercalation). Electrolyte reduction is restricted to the first few cycles until an effective (pin-hole free, electronically insulating, Li^+-cation conducting, and dimensionally stable during cycling) SEI is formed (Fig. 7a).

By contrast, the metal anode/electrolyte interface is quite variable during cycling, due to the large volume changes. The once formed film may break up, and parts of it may even break off. Whenever fresh, unfilmed surface of the active material is exposed to the electrolyte, a new SEI will be formed (Fig. 7b). Hence, filming will extend over a larger number of cycles, maybe all throughout cycling. The ideal SEI for lithium storage metals and alloys is therefore a thin one, which is associated with a minimum of lithium and electrolyte loss, and a flexible one, which can better withstand the volume changes during cycling. Though the reversible capacities (discharge capacities) and the cycling stability of the metal host anodes

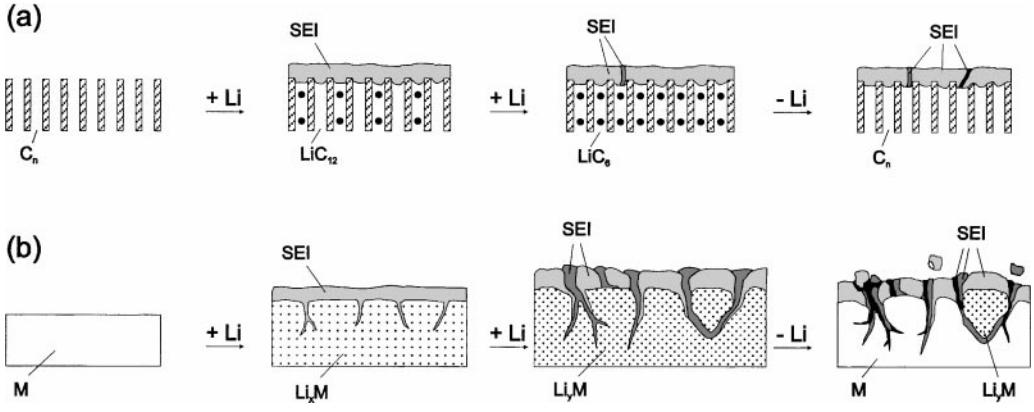

Fig. 7. Model for SEI formation on (a) carbonaceous and (b) metallic host materials; different shading of the SEI indicate SEI formed at different stages of Li uptake and release (not different composition)

[6] It should be noted that this model is simplified, as it does not consider, for instance, effects caused by the changing morphology (which influences the electrode kinetics), by the increasing electrode impedance (which results from film growth), or a break-up of the SEI during discharge which is followed by new film formation (at the expense of Li, which is extracted from the metal/intermetallic), *etc*.

[7] For the present electrode and cell design and cycling mode.

are quite good, both the electrolyte composition and the metal anode surface have not been optimized with respect to adequate SEI formation. This task is subject to present investigations.

Experimental

Synthesis of lithium storage alloys

The nanocrystalline Sn/SnSb and Ni(B) powders were precipitated with $NaBH_4$ from aqueous solutions of the respective chlorides (the former in the presence of complexants). The particle size of the Sn/SnSb powder was below 300 nm, the *BET* surface area was $14.5\,m^2\,g^{-1}$, the nominal composition was $Sn_{0.88}Sb_{0.12}$, and the Ni(B) powder contained approximately 8% (w/w) B. Further details on the synthesis of the powders can be found elsewhere [19].

Electrolytes, electrodes, and cells

ES (Aldrich, 98%) was distilled under vacuum. *EC*, *PC*, *DMC*, and $LiClO_4$ (all Merck, battery grade) were used as received. $LiN(SO_2CF_3)_2$ (3 *M*) was dried under dynamic vacuum at 110°C for 48 h. *BTE* was synthesized and purified as described in Ref. [18]. All electrolyte components (solvents and electrolyte salts) were handled by standard procedures (*e.g.* Refs. [8, 13]). The ratios of the solvents in the electrolyte mixtures are given in volume percent. The water content of the electrolytes was typically less than 15 ppm as determined by *Karl Fischer* titration. Graphite based composite anodes were made from TIMREX® graphites and 5% (w/w) polyvinylidene fluoride (*PVDF*) binder as described elsewhere [8]. Composite lithium storage alloy electrodes were prepared by pasting a well-mixed slurry of 82% (w/w) Sn/SnSb, 10% Ni(B), and 8% *PVDF* onto stainless steel mesh, pre-drying, pressing, and final drying in vacuum at 120–140°C (for more details, see Ref. [19]). Electrolyte preparation and cell assembly were accomplished under a dry argon atmosphere in a glove box. Electrochemical experiments were carried out in laboratory type glass cells with bulk lithium counter and reference electrodes and an excess of electrolyte. The electrodes were not closely packed in separator materials but placed in the electrolyte without any further support or protection. The constant current charge/discharge and voltammetric experiments were performed with ADESYS electrochemical testing units developed in our laboratory [28].

Acknowledgements

Financial support by the *Austrian Science Foundation* and the *OeNB* within the special research program *Electroactive Materials* and Project No. FWF-P12768-CHE is gratefully acknowledged. The work on lithium storage alloys is supported by Mitsubishi Chemical Corp. (Japan). Merck KGaA (Germany) and the TIMCAL group (Switzerland) have provided samples used in this study.

References

[1] Nagaura T, Tozawa K (1990) Prog Batt Solar Cells **9**: 209
[2] Nomura Research Institute (1996) Nomura Institute Research Report, Advanced Rechargeable Battery Industry '96, Tokyo, Japan
[3] See for example papers in: ITE Batt Lett (1999) Vol 1(2)
[4] Winter M, Besenhard JO, Spahr ME, Novák P (1998) Adv Mater **10**: 725
[5] Winter M, Besenhard JO (1999) Lithiated Carbons. In: Besenhard JO (ed) Handbook of Battery Materials, part III. Wiley-VCH, Weinheim, p 383
[6] Winter M, Besenhard JO (1999) Electrochim Acta **45**: 31

[7] Peled E, Golodnitzky D, Penciner J (1999) The Anode/Electrolyte Interface. In: Besenhard JO (ed) Handbook of Battery Materials, part III. Wiley-VCH, Weinheim, p 419
[8] Wrodnigg GH, Besenhard JO, Winter M (1999) J Electrochem Soc **146**: 470
[9] Besenhard JO, Wagner MW, Winter M, Jannakoudakis AD, Jannakoudakis PD, Theodoridou E (1993) J Power Sources **43–44**: 413
[10] Imhof R, Novák P (1996) J Electrochem Soc **145**: 1081
[11] Wrodnigg GH, Wrodnigg TM, Besenhard JO, Winter M (1999) Electrochem Comm **1**: 148
[12] Wrodnigg GH, Reisinger C, Besenhard JO, Winter M (1999) ITE Batt Lett **1**: 110
[13] Lie LH, Hodal T, Möller KC, Wrodnigg GH, Appel WK, Besenhard JO, Winter M (1999) ITE Batt Lett **1**: 106
[14] Möller KC, Hodal T, Appel WK, Besenhard JO, Winter M (to be published)
[15] Besenhard JO, v. Werner K, Winter M (1997) Ger Pat PCT/DE97/107506.4-1215 Eur Pat 807986, US Pat 5916708
[16] Appel WK, Besenhard JO, Pasenok S, Winter M, Wrodnigg GH (1998) Ger Offen DE 19 724 709 Al
[17] Appel WK, Besenhard JO, Lie LH, Pasenok S, Winter M (1998) Eur Patent Appl
[18] Appel WK, Besenhard JO, Lie LH, Pasenok S, Winter M (1998) Eur Patent Appl
[19] Yang J, Wachtler M, Winter M, Besenhard JO (1999) Electrochem Solid-State Lett **2**: 161
[20] Besenhard JO, Yang J, Winter M (1997) J Power Sources **68**: 87
[21] Yang J, Winter M, Besenhard JO (1996) Solid State Ionics **90**: 281
[22] Boukamp BA, Lesh GC, Huggins RA (1981) J Electrochem Soc **128**: 725
[23] Idota Y, Kubota T, Matsufuji A, Maekawa Y, Miyasaka T (1997) Science **276**: 1395
[24] Courtney IA, Dahn JR (1997) J Electrochem Soc **144**: 2045
[25] Mao O, Turner RL, Courtney IA, Fredericksen BD, Buckett MI, Krause LJ, Dahn JR (1999) Electrochem Solid-State Lett **2**: 3
[26] Courtney IA, McKinnon WR, Dahn JR (1999) J Electrochem Soc **146**: 59
[27] Yang J, Besenhard JO, Winter M (1997) In: Holmes CF, Landgrebe AR (eds) The Electrochemical Society Proceedings Series 97-18, Batteries for portable applications and electric vehicles, p 350
[28] Evers B, Schneider I, Wrodnigg GH, Winter M, Besenhard JO (March 31, 1998) In: Schwabe I (ed) Begleittexte zum Entwicklerforum: Batterien, Ladekonzepte & Stromversorgungsdesign. München, p 28

Received May 30, 2000. Accepted June 14, 2000